

Enhancement of the critical current density in single-crystal $\text{Bi}_2\text{Sr}_2\text{CaCu}_2\text{O}_8$ superconductors by chemically induced disorder

(metal substitution/defects/scanning tunneling microscopy/superstructure)

YUE LI WANG, XIAN LIANG WU, CHIA-CHUN CHEN, AND CHARLES M. LIEBER*

Department of Chemistry, Columbia University, New York, NY 10027

Communicated by Nicholas J. Turro, June 28, 1990 (received for review May 30, 1990)

ABSTRACT The effect of metal substitution on the critical current densities of single-crystal $\text{Pb}_x\text{Bi}_{2-x}\text{Sr}_2\text{CaCu}_2\text{O}_8$ ($x = 0$ or $x = 0.7$) superconductors has been investigated. Substitution of lead was found to increase the average critical current density from $1 \times 10^5 \text{ A/cm}^2$ to $2 \times 10^6 \text{ A/cm}^2$ at 5 K in an applied magnetic field of 10 kilooersteds (1 oersted = 80 A/m). The order of magnitude increase in the critical current density was observed for temperatures up to the flux vortex lattice melting point; the flux lattice melting point was also found to increase to 30 K (from 22 K) in the lead-substituted materials. Diffraction and microscopy investigations of the structural parameters indicate that the fundamental atomic lattices are virtually the same for both materials. Scanning tunneling microscopy images demonstrate, however, that lead substitution causes significant disorder (or defects) in the one-dimensional superstructure found in $\text{Bi}_2\text{Sr}_2\text{CaCu}_2\text{O}_8$. Since crystal defects can increase the critical current density by pinning the motion of flux vortices, it is likely that this lead-induced disorder enhances vortex pinning. The lead-induced disorder is specific to the nonsuperconducting Bi–O layers, and thus our results suggest that chemical substitutions may be utilized to control selectively flux pinning and the critical current density in these materials.

High bulk critical current densities (J_c values) are essential to many proposed applications of high-temperature copper oxide superconductors. Hence, a major focus of research in this field has been to develop materials with improved values of J_c . In general, the introduction of “defects” into the crystal lattice [for example, by neutron (1, 2) and ion irradiation (3), shock compression (4), or precipitation (5, 6)] has often resulted in increased values of J_c . Such increases in J_c are due to enhanced pinning of the motion of flux vortices by defects, although for the most part the nature of the defects is not well understood. To better understand and to control the nature of defects and flux pinning in these materials, we have been exploring chemical approaches for selectively creating defects and herein report studies of both J_c and the microstructure for high-quality single crystals of Pb-substituted $\text{Bi}_2\text{Sr}_2\text{CaCu}_2\text{O}_8$ superconductors.

To investigate J_c and possible defect structures in bulk $\text{Bi}_2\text{Sr}_2\text{CaCu}_2\text{O}_8$ materials, we have chosen to study single-crystal samples since the intrinsic composition, structure, electrical, and magnetic properties can be more accurately determined in high-quality crystals than in ceramic samples. Single crystals with a nominal stoichiometry $\text{Pb}_x\text{Bi}_{2-x}\text{Sr}_2\text{CaCu}_2\text{O}_8$, where $x = 0$ or $x = 0.7$, were grown from copper oxide-rich melts (7, 8). Briefly, a mixture of PbO , Bi_2O_3 , SrCO_3 , CaCO_3 , and CuO powders was melted at 980°C , cooled at 2°C/hr to 800°C , and then furnace cooled to room temperature. The typical Pb:Bi:Sr:Ca:Cu ratios used for the

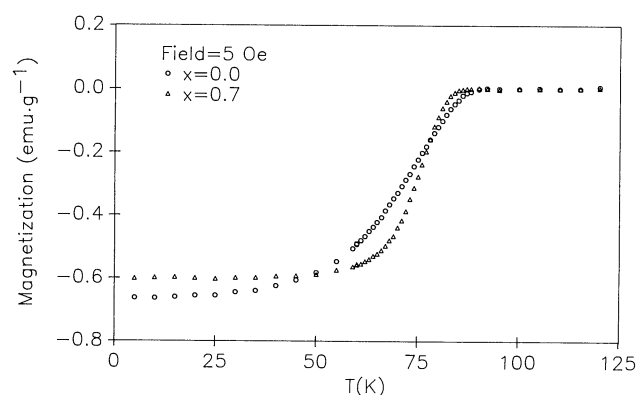


FIG. 1. Magnetization curves recorded by cooling $x = 0$ and $x = 0.7$ crystals in a field of 5 Oe. The magnetic field was aligned perpendicular to the a – b crystal plane. For the $x = 0$ sample, the critical transition temperature (T_c) = 86 K, while for the $x = 0.7$ crystal, T_c = 83 K; the superconducting fractions are similar in both samples.

synthesis of $x = 0$ and $x = 0.7$ samples were 0:2:2:1:2.2 and 0.85:1.15:2:1:2.2, respectively. Bulk analyses of the resulting crystals demonstrate that the $x = 0$ and $x = 0.7$ crystals have a similar Bi or Pb + Bi, Sr, Ca, and Cu stoichiometry: $\text{Bi}_{2.1}\text{Sr}_{1.8}\text{Ca}_{0.7}\text{Cu}_{1.8}\text{O}_x$ and $\text{Pb}_{0.7}\text{Bi}_{1.4}\text{Sr}_{1.6}\text{Ca}_{0.7}\text{Cu}_{1.8}\text{O}_x$. Auger electron spectroscopy of $x = 0.7$ samples also shows that the surface Pb:Bi ratio is similar to the bulk stoichiometry and essentially constant when a crystal is repeatedly cleaved. Furthermore, single-crystal x-ray diffraction studies show that the crystal structures of the $x = 0$ and $x = 0.7$ materials are nearly identical. These results, which are in agreement with previous reports (9–11), indicate that Pb substitutes primarily for Bi and does not, for example, precipitate between the Bi–O/Bi–O double layers in this material.

The average values of the critical transition temperature for the $x = 0$ and $x = 0.7$ materials determined from dc four-probe resistivity measurements are 85 ± 4 and 85 ± 2 K (mean \pm SD), respectively; the resistive transition widths are small ($\approx 3^\circ$) and indicative of high-quality materials. Low-field magnetic flux expulsion measurements on these materials were made by using a superconducting quantum interference device (SQUID)-based magnetometer (MPMS, Quantum Design, San Diego). These results (Fig. 1) demonstrate that the $x = 0$ and $x = 0.7$ materials have similar bulk superconducting fractions and appear to be single phase. The magnetic measurements also confirm that the critical transition temperatures are nearly the same for the $x = 0$ and $x = 0.7$ materials.

We have determined J_c in these samples from measurements of the magnetization hysteresis loops. Typical hysteresis loops recorded with the applied magnetic field perpen-

The publication costs of this article were defrayed in part by page charge payment. This article must therefore be hereby marked “advertisement” in accordance with 18 U.S.C. §1734 solely to indicate this fact.

Abbreviations: SQUID, superconducting quantum interference device; STM, scanning tunneling microscopy.

*To whom reprint requests should be addressed.

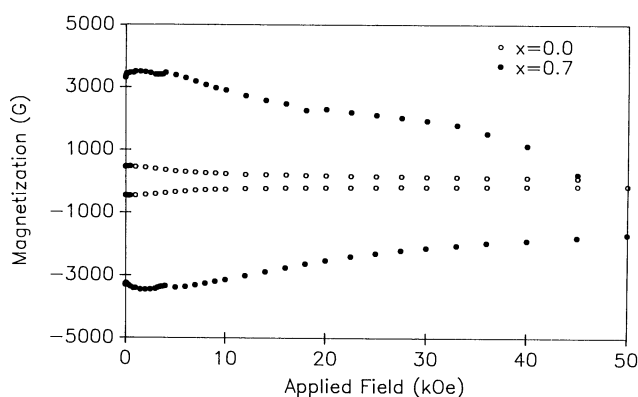


FIG. 2. Magnetization hysteresis loops recorded for $x = 0$ ($0.15 \times 0.11 \times 0.012 \text{ cm}^3$ sample) and $x = 0.7$ ($0.17 \times 0.09 \times 0.005 \text{ cm}^3$ sample) crystals at 5 K with the field perpendicular to the plane (a - b) defined by the two larger dimensions of the rectangular crystals. The samples were cycled between 50 kOe and -50 kOe before recording the hysteresis loops. The large difference in the magnitude of the hysteresis indicates that flux vortices are pinned more effectively in the $x = 0.7$ vs. $x = 0$ sample.

dicular to the a - b plane of $x = 0$ and $x = 0.7$ crystals are shown in Fig. 2. The hysteresis loops were determined by measuring the magnetization at discrete values of applied magnetic field with the SQUID magnetometer; the time between points was typically 8 min. It is immediately obvious that the magnetization loop for the $x = 0.7$ crystal has significantly greater hysteresis than the loop determined for the $x = 0$ crystal; that is, enhanced flux pinning is observed. Using the critical-state model for strongly pinned type II superconductors as developed by Bean (12), we have analyzed our magnetization data in the standard way to determine J_c (2). For a rectangular sample of width w and length l , $J_c = (20\Delta M/w)/(1 - w/3l)$, where ΔM is the hysteresis in the magnetization for a specific applied field. We find at 5 K in an applied field of 10 kilooersted (kOe; 1 Oe = 80 A/m) that $J_c = 1.6 \times 10^6 \text{ A/cm}^2$ for the $x = 0.7$ sample and that $J_c = 1.2 \times 10^5 \text{ A/cm}^2$ for the $x = 0$ sample. These data demonstrate that Pb substitution enhances J_c by more than an order of magnitude for crystals grown using virtually identical conditions.

In addition, we find that this 10-fold enhancement of J_c is reproducible. Analysis of magnetization loops measured on six independent $x = 0.7$ and $x = 0$ crystals at 5 K and 10 kOe yields average values for J_c of 2×10^6 and $1 \times 10^5 \text{ A/cm}^2$, respectively. These measurements were made on samples having different physical sizes, and furthermore, the crystals

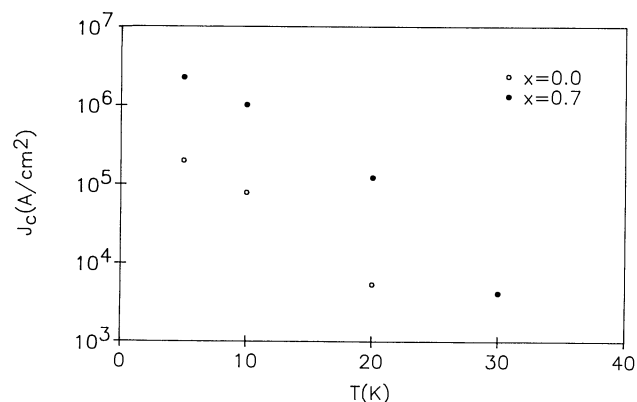


FIG. 3. Temperature dependence of the critical current density in an applied field of 4 kOe for $x = 0$ and $x = 0.7$ materials. The critical current densities were determined from magnetization hysteresis loops as described in the text.

were obtained from independent growth runs. Hence, we believe that our results are representative of the intrinsic J_c values of these materials. We note that these measurements represent a lower limit of J_c since the magnetization decays during the time required to measure each point in a given hysteresis loop (13). The order of magnitude enhancement of J_c is also observed at higher temperatures as shown in Fig. 3. Furthermore, the data from these temperature-dependence studies show that the flux lattice in the $x = 0.7$ crystals melts (i.e., the magnetization hysteresis collapses to 0) at a higher

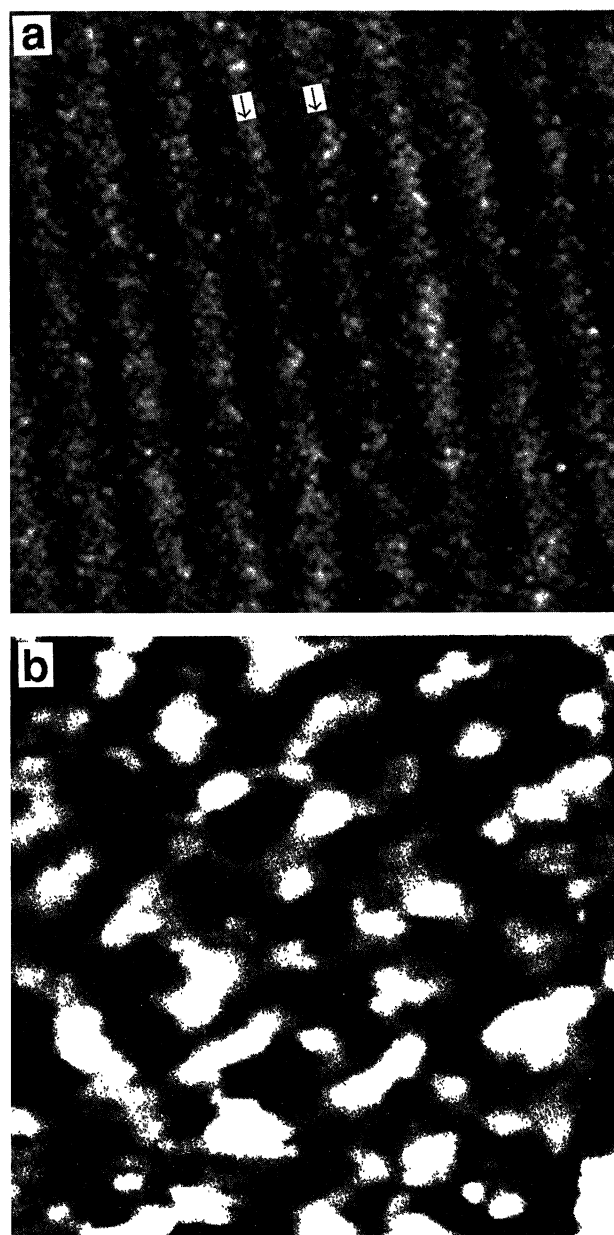


FIG. 4. Unfiltered $200 \times 200 \text{ Å}^2$ gray-scale STM images of single crystals of $\text{Bi}_2\text{Sr}_2\text{CaCu}_2\text{O}_8$ (a) and $\text{Pb}_{0.7}\text{Bi}_{1.3}\text{Sr}_2\text{CaCu}_2\text{O}_8$ (b) recorded in the constant current mode with a commercial instrument (Nanoscope, Digital Instruments, Santa Barbara, CA, ref. 8). The bias voltage and tunneling current were 250 mV and 0.6 nA for a and 400 mV and 0.8 nA for b. The lighter areas in these images correspond to apparent surface protrusions. A prominent one-dimensional superstructure of period 25 Å is visible in a; two modulation maxima are denoted with arrows. In the image of the $x = 0.7$ sample (b) this superstructure is, however, highly distorted; the modulation amplitude of the large-scale structure in this image is also 4 times greater than in a.

temperature (30 vs. 22 K) than in the $x = 0$ material (14, 15). Although the flux lattice melting temperature in the $x = 0.7$ material (30 K) is still too low for practical applications, the observed increase in melting temperature suggests that additional work may raise this value further.

It is reasonable to attribute the significant increase in J_c for the $x = 0.7$ crystals to defects that enhance the pinning of flux vortex motion relative to the $x = 0$ materials, although the exact nature of these defects remains in question. In general, previous studies of modified materials exhibiting enhanced J_c values have not reported the nature of such defects (1–3, 6), although recently it has been suggested for crystallized BiSrCaCuO glasses that nonsuperconducting Ca and Cu precipitates may effectively pin flux motion (5). Our compositional and structural measurements for the $x = 0$ and $x = 0.7$ crystals, as well as other reported studies (8–11), indicate that Pb (or other) precipitates are unlikely in these single crystals. To elucidate the nature of the defects that enhance J_c in the $x = 0.7$ materials, we have concentrated on directly examining the microstructural effects of Pb substitution in real space by scanning tunneling microscopy (STM). STM is an ideal technique for characterizing the structural effects of Pb substitution since Pb primarily replaces Bi in the Bi–O layers (9, 10) and $\text{Pb}_x\text{Bi}_{2-x}\text{Sr}_2\text{CaCu}_2\text{O}_8$ crystals cleave to expose a Bi(Pb)–O layer (8, 16). Thus, in the STM experiment, we directly image the layer into which Pb has been substituted.

As discussed elsewhere in detail (8), we find that on an atomic scale the structure of the Bi(Pb)–O layer is virtually unchanged in the $x = 0.7$ versus the $x = 0$ samples. Specifically, there is neither a dramatic increase in site vacancies nor highly localized distortions of the lattice, and thus we conclude it is unlikely that atomic scale point defects are the cause of the enhancements in J_c . However, large-scale STM images show that Pb substitution disorders the one-dimensional superstructure found in $\text{Bi}_2\text{Sr}_2\text{CaCu}_2\text{O}_8$ (8, 16, 17) (Fig. 4). Images of $x = 0.7$ crystals show only a random modulation in the Bi(Pb)–O layer compared to the regular one-dimensional superlattice (period ≈ 25 Å) observed in the $x = 0$ image. Additionally, the average magnitude of the modulation, which may reflect a combination of structural and electronic effects (18), is 3.8 times larger (average of 10 independent images) in the $x = 0.7$ than in the $x = 0$ crystals. It is likely that the larger disorder and greater amplitude of this modulation in the Pb-substituted samples enhance vortex pinning in these materials.

It is also interesting to note that our structural studies indicate that Pb-induced defects are localized in the Bi–O layer of this material. In contrast, the defects produced by neutron and ion irradiation of materials are randomly distributed throughout the sample volume. This point is partic-

ularly important since defects in the Cu–O layer will rapidly decrease the critical transition temperature. Hence, chemical substitution offers the unique possibility of selectively introducing defects into non-Cu–O layers (e.g., Pb in the Bi–O layer) so that these defects do not adversely affect the superconducting transition temperature yet still enhance J_c .

We thank Y. Uemura, G. Luke, and B. Sternlieb for generous use of the SQUID-based magnetometer and M. Vernon, D. Ginley, G. Venturini, B. Morosin, and R. Baughman for helpful discussions. C.M.L. acknowledges support of this work by the David and Lucile Packard Foundation.

1. Umezawa, A., Crabtree, G. W., Liu, J. Z., Weber, H. W., Kwok, W. K., Nunez, L. H., Moran, T. J., Sowers, C. H. & Claus, H. (1987) *Phys. Rev.* **36**, 7151–7154.
2. van Dover, R. B., Gyorgy, E. M., Schneemeyer, L. F., Mitchell, J. W., Rao, K. V., Puzniak, R. & Waszczak, J. V. (1989) *Nature (London)* **342**, 55–57.
3. Roas, B., Hensel, B., Saemann-Ischenko, G. & Schultz, L. (1989) *Appl. Phys. Lett.* **54**, 1051–1053.
4. Murr, L. E., Niou, C. S., Jin, S., Tiefel, T. H., James, A. C. W. P., Sherwood, R. C. & Siegrist, T. (1989) *Appl. Phys. Lett.* **55**, 1575–1577.
5. Shi, D., Boley, M. S., Welp, U., Chen, J. G. & Liao, Y. (1989) *Phys. Rev.* **40**, 5255–5258.
6. Dou, S. X., Guo, S. J., Liu, H. K. & Easterling, K. E. (1989) *Supercond. Sci. Technol.* **2**, 308–310.
7. Bukowski, E. D. & Ginsberg, D. M. (1989) *J. Low Temp. Phys.* **77**, 285–291.
8. Wu, X. L., Zhang, Z., Wang, Y. L. & Lieber, C. M. (1990) *Science* **248**, 1211–1214.
9. Ramesh, R., Thomas, G., Green, S. M., Jiang, C., Mei, Y., Rudee, M. L. & Lou, H. L. (1988) *Phys. Rev.* **38**, 7070–7073.
10. Ramesh, R., Hegde, M. S., Chang, C. C., Tarascon, J. M., Green, S. M. & Luo, H. L. (1989) *J. Appl. Phys.* **66**, 4878–4885.
11. Schneek, J., Pierre, L., Toledano, J. C. & Daguet, C. (1989) *Phys. Rev.* **39**, 9624–9627.
12. Bean, C. P. (1962) *Phys. Rev. Lett.* **8**, 250–253.
13. Yeshurun, Y. & Malozemoff, A. P. (1988) *Phys. Rev. Lett.* **60**, 2202–2205.
14. Ansaldo, E. J., Batlogg, B., Cava, R. J., Harshman, D. R., Rupp, L. W., Riseman, T. M. & Williams, D. (1989) *Physica C* **162**, 259–260.
15. van Dover, R. B., Schneemeyer, L. F., Gyorgy, E. M. & Waszczak, J. V. (1988) *Appl. Phys. Lett.* **52**, 1910–1912.
16. Kirk, M. D., Nogami, J., Baski, A. A., Mitzi, D. B., Kapitlnik, A., Geballe, T. H. & Quate, C. F. (1988) *Science* **242**, 1673–1675.
17. Shaw, T. M., Shivashankar, S. A., La Placa, S. J., Cuomo, J. J., McGuire, T. R., Roy, R. A., Kelleher, K. H. & Yee, D. S. (1988) *Phys. Rev.* **37**, 9856–9859.
18. Wu, X. L., Zhou, P. & Lieber, C. M. (1988) *Nature (London)* **335**, 55–56.